ЖЭТФ, 2014, том 145, вып. 5, стр. 906–922 © 2014

OPTICAL DEFECT MODES AT AN ACTIVE DEFECT LAYER IN PHOTONIC LIQUID CRYSTALS

V. A. Belyakov[a]*, S. V. Semenov*[b]

[a] *Landau Institute for Theoretical Physics, Russian Academy of Sciences 142432, Chernogolovka, Moscow Region, Russia*

[b] *National Investigation Centre «Kurchatov Institute» 123182, Moscow, Russia*

Received October 10, 2013

An analytic approach to the theory of the optical defect modes in photonic liquid crystals in the case of an active defect layer is developed. The analytic study is facilitated by the choice of the problem parameters related to the dielectric properties of the studied structures. The chosen models allow eliminating polarization mixing at the external surfaces of the studied structures. The dispersion equations determining the relation of the defect mode (DM) frequency to the dielectric characteristics of an isotropic, birefringent and absorbing (amplifying) defect layer and its thickness are obtained. Analytic expressions for the transmission and reflection coefficients of the defect mode structure (DMS) (photonic liquid crystal–active defect layer–photonic liquid crystal) are presented and analyzed. The effect of anomalously strong light absorption at the defect mode frequency for an absorbing defect layer is discussed. It is shown that in a distributed feedback lasing at the DMS with an amplifying defect layer, adjusting the lasing frequency to the DM frequency results in a significant decrease in the lasing threshold and the threshold gain decreases as the defect layer thickness increases. It is found that generally speaking the layer birefringence and dielectric jumps at the interfaces of the defect layer and photonic liquid crystal reduce the DM lifetime in comparison with the DMS with an isotropic defect layer without dielectric jumps at the interfaces. Correspondingly, generally speaking, the effect of anomalously strong light absorption at the defect mode frequency and the decrease in the lasing threshold are not so pronounced as in the case of the DMS with an isotropic defect layer without dielectric jumps at the interfaces. The case of a DMS with a low defect layer birefringence and sufficiently large dielectric jumps are studied in detail. The options of effectively influencing the DM parameters by changing the defect layer dielectric properties, and the birefringence in particular, are discussed.

DOI: 10.7868/S0044451014050139

1. INTRODUCTION

The field of mirrorless distributed feedback (DFB) lasing in photonic structures consisting of many layers of chiral liquid crystals was recently attracting much attention, mainly due to the possibilities of reaching a low lasing threshold for DFB lasing [1–8]. For definiteness, we study photonic liquid crystals with the example of the best known type of photonic liquid crystals, cholesteric liquid crystals (CLC). The related theory is mostly based on numerical calculations [9], whose results are not always interpreted in the framework of a clear physical picture. Several recent papers [10–15] showed that an analytic theoretical approach to the problem (sometimes limited by the introduced approximations) allows creating a clear physical picture of linear optics and lasing in the relevant structures. In particular, the physics and the role of localized optical modes (edge and defect modes) in the structures under consideration was clearly demonstrated. The most promising results in DFB lasing relate to defect modes (DM) [12, 13]. The defect modes existing at a structure defect as a localized electromagnetic eigenstate with its frequency in the forbidden band gap were investigated initially in the three-dimensionally periodic dielectric structures [16]. The corresponding defect modes in chiral liquid crystals and, more generally, in spiral media are very similar to the defect modes in one-dimensional scalar periodic structures. They reveal abnormal re-

*E-mail: bel@landau.ac.ru

flection and transmission inside the forbidden band gap [1, 2] and allow DFB lasing at a low lasing threshold [3]. The qualitative difference from scalar periodic media consists in the polarization properties. The defect mode in chiral liquid crystals is associated with a circular polarization of an electromagnetic field eigenstate with the chirality sense coinciding with the one of the chiral liquid crystal helix. There are two main types of defects in chiral liquid crystals studied up to now. One is a plane layer of some substance differing from the CLC, dividing a perfect cholesteric structure into two parts, and being perpendicular to the helical axis of the cholesteric structure [1]. The other defect type is a jump of the cholesteric helix phase at some plane perpendicular to the helical axis (without insertion of any substance at the location of this plane) [2]. Recently, many new types of defect layers were studied [17–23], for example, a CLC layer with the pitch differing from the pitch of two layers sandwiched between these layers [8]. It is evident that there are many versions of the dielectric properties of the defect layer, but the consideration below is limited by the first type of defect, a layer inserted into a chiral liquid crystal. Our focus is on the active defect layer (absorbing, amplifying or changing light polarization). The reason for that is connected with both experimental research on the DFB lasing in CLCs where dyes are placed in a defect layer [24] and the general idea that the unusual properties of the DM manifest themselves most clearly just at the middle of the defect structure, i. e., at the defect layer, where the DM field intensity reaches its maximum. We therefore assume that there is no absorption in the CLC layers of the DMS, and absorption, amplification or changes of light polarization occur only in the defect layer. The analytic approach to studying a DMS with an active defect layer is very similar to the previously performed DM studies [12, 13], and we therefore present the final results of the present investigation, referring the reader to [12, 13] for the investigation details.

In this paper, an analytic solution for the defect mode associated with an insertion of an active defect layer into the perfect cholesteric structure is presented for light propagating along the helical axis and some limit cases simplifying the problem are considered.

2. DEFECT MODE AT AN AMPLIFYING (ABSORBING) DEFECT LAYER

To consider the DM associated with an insertion of an isotropic layer into a perfect cholesteric structure,

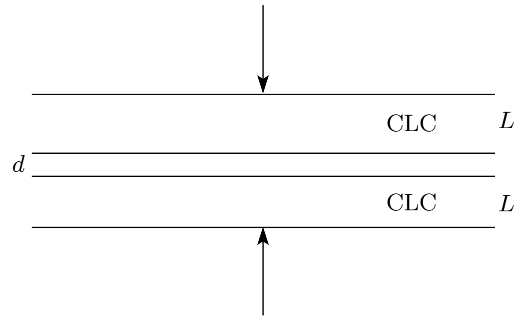

Fig. 1. Schematic of the CLC defect mode structure with an isotropic active defect layer of thickness d

we have to solve the Maxwell equations and a boundary value problem for the electromagnetic wave propagating along the cholesteric helix for the layered structure depicted in Fig. 1. This investigation was performed in [12, 13] under the assumption that the CLC layers can be absorbing or amplifying in Fig. 1. It is possible to use the results in [12, 13] in the present case of an amplifying (absorbing) isotropic defect layer and non-absorbing CLC layers introducing only some physically clear changes in the formulas obtained in [12, 13]. The assumptions in [12, 13], that the average dielectric constant of CLC ε_0 coincides with the dielectric constant of the defect layer and the external medium, and hence polarization conversion at the interfaces is absent and only light of diffracting circular polarization has to be taken into account, are retained in this section. The main conventions and notation of papers [12, 13] are also preserved in this section. As is known [9], much information on the DM is available from spectral properties of the defect mode structure (DMS) transmission $T(d, L)$ and reflection $R(d, L)$ coefficients.

Formulas for the optical properties of the structure depicted at Fig. 1 can be obtained using the expressions for the amplitude transmission $T(L)$ and reflection $R(L)$ coefficient for a single cholesteric layer (see also [25, 26]). The transmission $|T(d, L)|^2$ and reflection $|R(d, L)|^2$ intensity coefficients (of light of the diffracting circular polarization) for the whole structure can be presented in the form

$$|T(d,L)|^2 = \left| \frac{T_e T_d \exp(ikd(1+ig))}{1 - \exp(2ikd(1+ig)) R_d R_u} \right|^2, \quad (1)$$

$$|R(d,L)|^2 = \left| R_e + \frac{R_u T_e T_u \exp(2ikd(1+ig))}{1 - \exp(2ikd(1+ig)) R_d R_u} \right|^2, \quad (2)$$

where $R_e(T_e)$, $R_u(T_u)$, and $R_d(T_d)$ are the respective amplitude reflection (transmission) coefficients of the individual CLC layer (see Fig. 1) for light incident at the outer top layer surface, at the inner top CLC layer surface from the inserted defect layer, and at the inner bottom CLC layer surface from the inserted defect layer. It is assumed in the deriving Eqs. (1) and (2) that the external beam is incident at the structure (Fig. 1) from above only. The factor $1 + ig$ is related to the defect layer only and corresponds to the dielectric constant of the defect layer having the form $\varepsilon_0(1 + 2ig)$ with a small g that is positive for an absorbing defect layer and negative for an amplifying one.

For completeness, we also present expressions for the amplitude transmission $T(L)$ and reflection $R(L)$ coefficients for a single nonabsorbing cholesteric layer of thickness L for light of diffracting circular polarization [25, 26]:

$$\begin{gathered} R(L) = i\delta \sin(qL) \left\{ \frac{q\tau}{\kappa^2} \cos(qL) + \right. \\ \left. + i \left[\left(\frac{\tau}{2\kappa}\right)^2 + \left(\frac{q}{\kappa}\right)^2 - 1 \right] \sin(qL) \right\}^{-1}, \\ T(L) = \exp\frac{i\tau L}{2} \frac{q\tau}{\kappa^2} \left\{ \frac{q\tau}{\kappa^2} \cos(qL) + \right. \\ \left. + i \left[\left(\frac{\tau}{2\kappa}\right)^2 + \left(\frac{q}{\kappa}\right)^2 - 1 \right] \sin(qL) \right\}^{-1}, \end{gathered} \tag{3}$$

where $\kappa = \omega\varepsilon_0^{1/2}/c$, $\tau = 4\pi/p$, p is the cholesteric pitch, $\varepsilon_0 = (\varepsilon_\parallel + \varepsilon_\perp)/2$, $\delta = (\varepsilon_\parallel - \varepsilon_\perp)/(\varepsilon_\parallel + \varepsilon_\perp)$ is the dielectric anisotropy, and $\varepsilon_\parallel$ and $\varepsilon_\perp$ are the local principal values of the liquid crystal dielectric tensor [25–29],

$$q = \kappa \left\{ 1 + (\tau/2\kappa)^2 - \left[(\tau/\kappa)^2 + \delta^2 \right]^{1/2} \right\}^{1/2}. \tag{4}$$

The defect mode frequency ω_D is determined by the dispersion equation

$$\begin{gathered} \exp\left(2ikd(1+ig)\right)\sin^2(qL) - \frac{\exp(-i\tau L)}{\delta^2} \times \\ \times \left[\frac{\tau q}{\kappa^2} \cos(qL) + i \left(\left(\frac{\tau}{2\kappa}\right)^2 + \left(\frac{q}{\kappa}\right)^2 - 1 \right) \sin(qL) \right]^2 = \\ = 0. \end{gathered} \tag{5}$$

For a finite thickness L of CLC layers, the DM frequency ω_D is a complex quantity, which can be found by solving Eq. (5) numerically. For very small values of the parameter g, the reflection and transmission spectra of an DMS with an active defect layer are similar to the spectra studied in [12, 13] (see Fig. 2). In particular, positions of dips in reflection and spikes in transmission inside the stop-band just correspond to $\mathrm{Re}\,\omega_D$, and this observation is very useful for numerically solving the dispersion equation. The DM lifetime is reduced for absorbing defect layers compared to a nonabsorbing defect layer [12, 13].

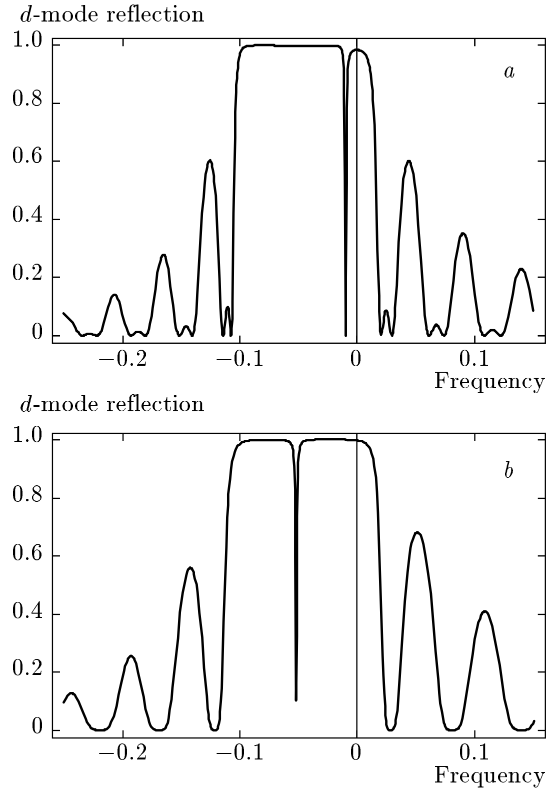

Fig. 2. Reflection $|R(d,L)|^2$ versus the frequency for a nonabsorbing defect and CLC layers ($g = 0$) at $d/p = 0.1$ (a), 0.25 (b); $l = 200$, $l = L\tau = 2\pi N$, where N is the director half-turn number at the CLC layer thickness L. Here and on figures below, $\delta = 0.05$, the director half-turn number at the CLC layer thickness is $N = 33$, frequency $\nu = \delta[2(\omega - \omega_B)/\delta\omega_B - 1]$

2.1. Absorbing defect layer

As in the case of investigated DMS with absorbing CLC layers [12, 13], the effect of anomalously strong absorption also occurs in DMS with absorbing defect layer. The effect reveals itself at the DM frequency and reaches its maximum (the maximum of $1 - |T(d,L)|^2 - |R(d,L)|^2$) for certain value of g that can be found using expressions (1) and (2) for $|T(d,L)|^2$ and $|R(d,L)|^2$. Figure 3 demonstrates the existence of the anomalously strong absorption effect at the DM frequency. As follows from Fig. 3, the maximum values of the anomalous absorption [25, 30] (the maximum of $1 - |T(d,L)|^2 - |R(d,L)|^2$) at two differing values of d/p are reached for $g = 0.04978$ and $g = 0.00008891$ (taken with the opposite sign, these are approximate values of g for the lasing threshold gain for the same DMSs).

In the case of thick CLC layers ($|q|L \gg 1$) in the DMS, the g value ensuring absorption maximum can be found analytically:

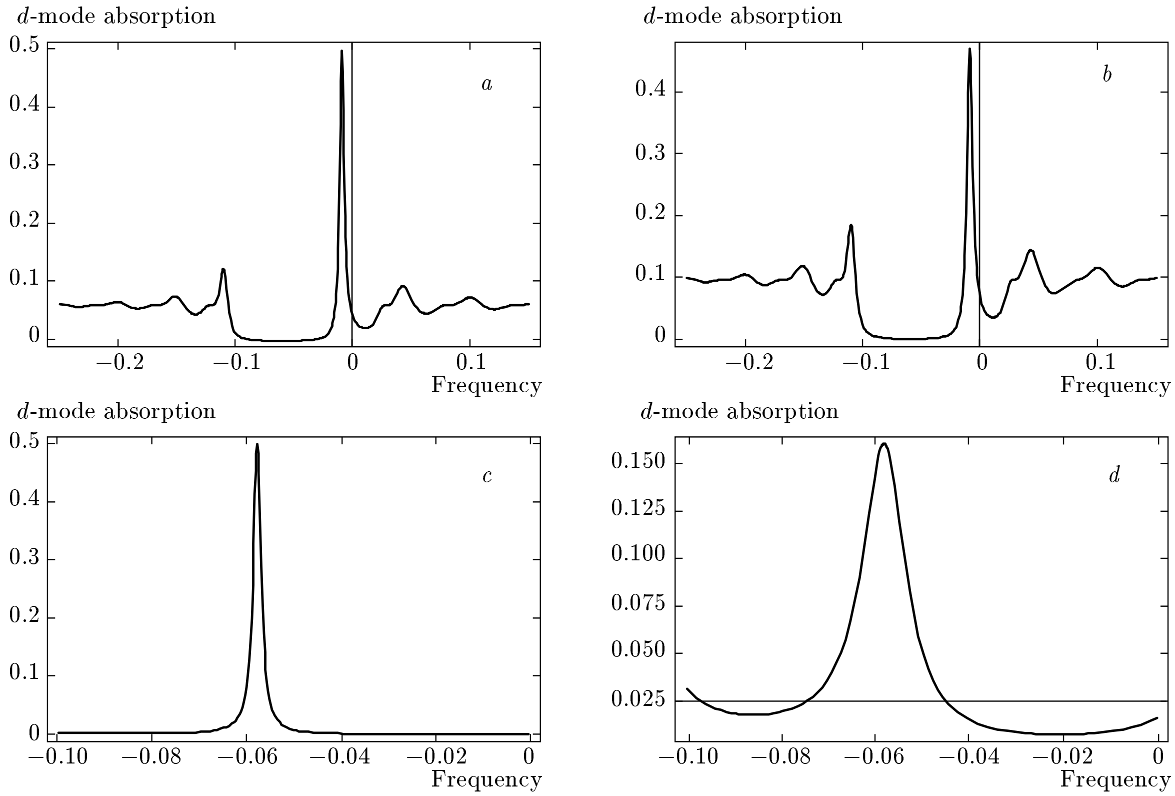

Fig. 3. Total absorption $1-|T(d,L)|^2-|R(d,L)|^2$ versus the frequency for an absorbing defect layer and nonabsorbing CLC layers at $g=0.04978$ (a), 0.08 (b) for $d/p=0.1$; at $g=0.00008891$ (c), 0.0008891 (d) for $d/p=22.25$

$$g_t=\frac{L}{d}\left|\frac{2\kappa^2}{q^2\tau L}\exp\left(-2|q|L\right)\times\left\{1+\frac{\left(2\left[(\tau/\kappa)^2+\delta^2\right]^{1/2}\right)^{-1}-(\tau/2\kappa)^2}{1-\left[(\tau/\kappa)^2+\delta^2\right]^{1/2}+(\tau/2\kappa)^2}\right\}^{-1}\right|. \quad (6)$$

For the defect mode frequency ω_D in the middle of the stop-band, the maximal absorption corresponds to

$$g_t=\frac{2}{3\pi}\,\frac{p}{d}\exp\left(-2\pi\delta\frac{L}{p}\right). \quad (7)$$

As the calculations and formulas (6) and (7) show, the gain g corresponding to the maximal absorption is approximately inversely proportional to the defect layer thickness d.

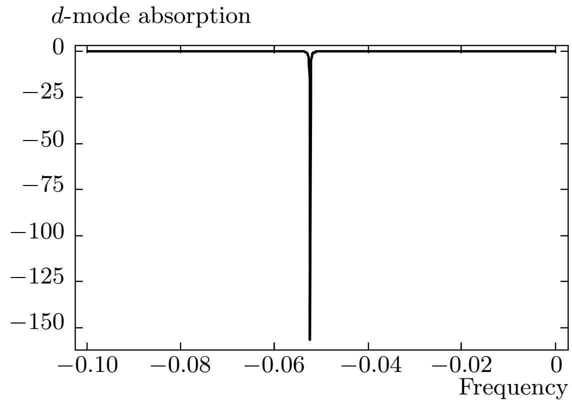

Fig. 4. Total absorption $1-|T(d,L)|^2-|R(d,L)|^2$ versus the frequency for an amplifying defect layer and nonabsorbing CLC layers at $g=-0.0065957$ for $d/p=0.25$

2.2. Amplifying defect layer

In the case of a DMS with an amplifying defect layer ($g<0$), the reflection and transmission coefficients diverge at some value of $|g|$. The corresponding values of g are the gain lasing thresholds. They can be found from dispersion equation (5) solved for g or numerically using expressions (1) and (2) for $|T(d,L)|^2$ and $|R(d,L)|^2$, or can be found approximately by plotting

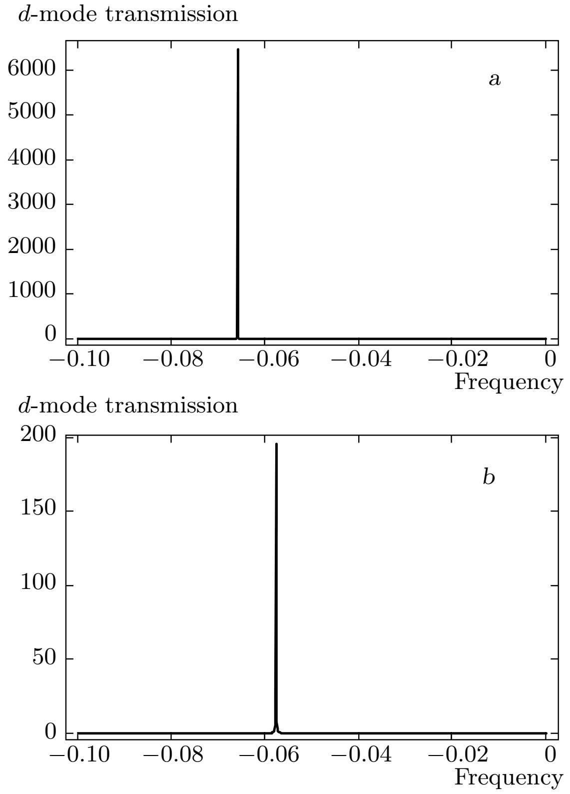

Fig. 5. Transmission $|T(d,L)|^2$ versus the frequency for an amplifying defect layer and nonabsorbing CLC layers at $g = -0.001000$ for $d/p = 2.25$ (a) and $g = -0.00008891$ for $d/p = 22.25$ (b)

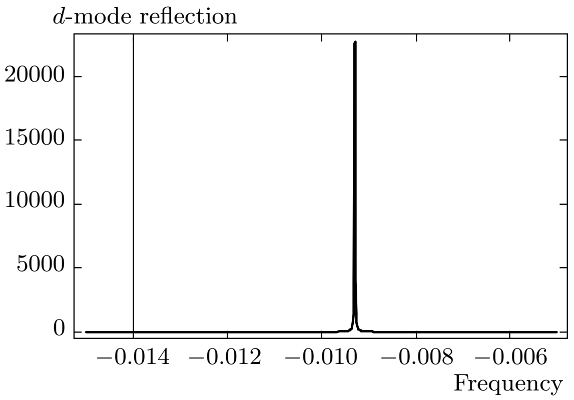

Fig. 6. Reflection $|R(d,L)|^2$ versus the frequency for an amplifying defect layer and nonabsorbing CLC layers at $g = -0.04978$ for $d/p = 0.1$

$|T(d,L)|^2$ and $|R(d,L)|^2$ as functions of g. The third option is illustrated by Figs. 4–6, where "almost divergent" values of $|T(d,L)|^2$, $|R(d,L)|^2$, or the absorption $1-|T(d,L)|^2-|R(d,L)|^2$ are shown. The used values of g in Figs. 4–6 are close to the threshold ones ensuring a divergence of $|T(d,L)|^2$ and $|R(d,L)|^2$. The calculation results show that the minimal threshold $|g|$ corresponds to the location of ω_D just in the middle of the stop-band and $|g|$ is almost inversely proportional to the defect layer thickness. Figures 4 and 5 actually correspond to the defect mode frequency ω_D located close to the middle point of the stop-band and demonstrate a decrease in the lasing threshold gain with an increase in the defect layer thickness. Figure 6 corresponds to the defect mode frequency ω_D located close to the stop-band edge and demonstrates an increase in the lasing threshold gain as the defect mode frequency ω_D approaches the stop band edge.

The analytic approach for thick CLC layers ($|q|L \gg 1$) results in similar predictions, namely, the gain threshold value is given by (6) with the negative sign of the right-hand side. For thick CLC layers with ω_D in the middle of the stop-band, the threshold gain is given by the expression

$$g_t = -\frac{2}{3\pi}\frac{p}{d}\exp\left(-2\pi\delta\frac{L}{p}\right). \qquad (8)$$

Hence, as formula (8) shows, the thinner the amplifying defect layer is, the higher threshold gain g.

The same result, as was mentioned above, is also valid for the absorption enhancement (formulas (6) and (7)). The thinner the absorbing defect layer is, the higher the g value ensuring maximal absorption.

An important result relating to DFB lasing at the DMS with an amplifying (absorbing) defect layer can be formulated as follows. The lasing threshold gain in a defect layer decreases as the amplifying layer thickness increases, being almost inversely proportional to the thickness. A similar result holds for the anomalously strong absorption phenomenon, where the value of g in the defect layer ensuring maximal absorption is almost inversely proportional to the defect layer thickness. We note that the revealed decrease in the lasing threshold gain with increasing the amplifying defect layer thickness cannot be regarded directly as the corresponding reduction in the lasing energy threshold of a pumping wave pulse. The situation depends on the specifics of pumping arrangement. This question requires a more thorough separate consideration. For example, if we assume that the pumping is arranged such that the gain g times the defect layer thickness d is proportional to the pumping pulse energy, then the threshold pumping pulse energy is almost independent of the defect layer thickness because of the almost inverse proportionality of the threshold gain to the defect layer thickness found above.

3. DEFECT MODE AT BIREFRINGENT DEFECT LAYER

The main attention in this section is paid to a birefringent defect layer and, in particular, to the case of low birefringence. As was already mentioned above, the reason for that is connected with both the experimental researches of DFB lasing in CLCs where the defect layer is birefringent [24] and the general idea that the unusual properties of the DM manifest themselves most clearly just at the middle of the defect structure, i. e., at the defect layer, where the DM field intensity reaches its maximum. We also assume from the beginning that there is no absorption in the CLC and the birefringent defect layer. The analytic approach in studying of a DMS with a birefringent defect layer is very similar to the previously performed DM studies for an isotropic defect layer [12, 13], and we therefore present the final results, referring the reader to [12, 13] for the details.

3.1. Nonabsorbing CLC layers

In this section, an analytic solution for the DM associated with an insertion of a birefringent defect layer in the perfect cholesteric structure is presented for light propagating along the helical axes and some limit cases simplifying the problem are considered. To consider the DM associated with the insertion of a birefringent layer in the perfect cholesteric structure, we have to solve the Maxwell equations and a boundary value problem for the electromagnetic wave propagating along the cholesteric helix for the layered structure with a birefringent defect layer depicted at Fig. 1. This investigation was already performed in [12, 13] under the assumption that the defect layer in Fig. 1 is isotropic. We can therefore use the results in [12, 13] for our case of a birefringent defect layer and nonabsorbing and amplifying (absorbing) CLC layers (keeping the notation of papers [12, 13] here), introducing only some physically clear changes in the formulas obtained in [12, 13]. The assumption in [12, 13] that the polarization conversion is absent and only light of diffracting circular polarization has to be taken into account (due to the assumption that the average CLC dielectric constant ε_0 coincides with the dielectric constant of the defect layer and the external medium) is not valid here. In fact, due to the birefringence of the defect layer, light polarization changes in the course of its propagation in the defect layer from one of its surfaces to the other, and hence, generally speaking, the polarization of light after crossing the defect layer differs from the polarization at the first defect layer surface. This is why the polarization component differing from the diffracting polarization occurs to be present in the DMS in general and the correspondingly polarized light leaks from the DMS. The evident consequence of this leakage is a reduction in the DM lifetime in the case of a birefringent defect layer.

Formulas for the optical properties of the structure with a birefringent defect layer depicted at Fig. 1 can be obtained using the expressions for the amplitude transmission $T(L)$ and reflection $R(L)$ coefficient for a single cholesteric layer in the presence of dielectric interfaces (see [25, 26]). If we neglect multiple scattering of nondiffracting polarization light, the transmission $|T(d,L)|^2$ and reflection $|R(d,L)|^2$ intensity coefficients (of light with the diffracting circular polarization) for the whole structure can be presented in the form

$$|T(d,L)|^2 = \left| \frac{T_e T_d M(k,d,\Delta n)(\boldsymbol{\sigma}_e \cdot \boldsymbol{\sigma}_{ed}^*)}{1 - M^2(k,d,\Delta n)(\boldsymbol{\sigma}_r \cdot \boldsymbol{\sigma}_{ed}^*)^2 R_d R_u} \right|^2, \quad (9)$$

$$|R(d,L)|^2 = \left| R_e + \frac{R_d T_e T_u M^2(k,d,\Delta n)|(\boldsymbol{\sigma}_e \cdot \boldsymbol{\sigma}_{ed}^*)|^2}{1 - M^2(k,d,\Delta n)(\boldsymbol{\sigma}_r \cdot \boldsymbol{\sigma}_{ed}^*)^2 R_d R_u} \right|^2, \quad (10)$$

where the meaning of $R_e(T_e)$, $R_u(T_u)$, and $R_d(T_d)$ is the same as in (1) and (2), and $\boldsymbol{\sigma}_e$, $\boldsymbol{\sigma}_r$, and $\boldsymbol{\sigma}_{ed}$ are the polarization vectors of light exiting the CLC layer inner surface, of light reflected at the inner bottom CLC layer surface at the incidence from the inserted defect layer, and of light whose some polarization vector $\boldsymbol{\sigma}_{ed}$ transforms to the polarization vector $\boldsymbol{\sigma}_e$ at crossing the birefringent defect layer of thickness d; Δn is the difference of two refractive indices in the birefringent defect layer and $M(k,d,\Delta n)$ is the phase factor related to the light single propagation in a birefringent defect layer. It is assumed in deriving Eqs. (9) and (10) that the external beam is incident at the structure (Fig. 1) from above only. In the presence of dielectric interfaces, there is light polarization conversion at the inner surfaces of CLC layers in DMS at reflection and transmission of light through a CLC layer and the light field inside CLC layers cannot be presented as a superposition of only two diffracting eigenmodes of the CLC (generally speaking, two nondiffracting eigenmodes are also present). The corresponding polarization vector inside the defect layer (after light crosses the interface between the CLC and defect layers), $\boldsymbol{\sigma}_e$, can be found (see [25, 26]), and the polarization vector $\boldsymbol{\sigma}_{ed}$ can be easily calculated if d and Δn are known. The same can be said about finding the polarization of light exciting diffracting eigenmodes in a CLC layer in its incidence at the external CLC layer surface in the DMS. The corresponding polarization in the presence of dielectric interfaces is called a diffracting polarization here. Polarization orthogonal to the diffracting polarization is here called the nondiffracting polarization. Light of a nondiffracting polarization being incident at a DMS excites only nondifracting CLC eigenmodes in CLC layers of the DMS. The polarization vectors $\boldsymbol{\sigma}_e$, $\boldsymbol{\sigma}_r$, and $\boldsymbol{\sigma}_{ed}$ can be presented in the form

$$\boldsymbol{\sigma}_i = (\cos\alpha_i \mathbf{e}_x + e^{i\beta_i}\sin\alpha_i \mathbf{e}_y), \tag{11}$$

where $\mathbf{e}_x$ and $\mathbf{e}_y$ are the unit vectors along the x and y axis, and α_i and β_i are the parameters determining the polarization. For example, $\alpha_i = \pi/4$ and $\beta_i = \pi/2(-\pi/2)$ corresponds to right (left) circular polarization.

In the general case for a DMS with a birefringent defect layer, the transmitted and reflected beams do not correspond to the diffracting circular polarization, and therefore there is reflection and transmission of the nondiffracting polarization light even for incident light of diffracting polarization. Neglecting multiple scattering of nondiffracting polarization light, we obtain the reflection $R(d,L)^-$ and transmission $T(d,L)^-$ coefficients of light of nondiffracting circular polarization (for incident light of diffracting circular polarization),

$$\begin{aligned}|T(d,L)^-|^2 = \Big|T_eT_d^-\{M(k,d,\Delta n)(\boldsymbol{\sigma}_e\cdot\boldsymbol{\sigma}_{ed}^{\perp *}) + \\ + (\boldsymbol{\sigma}_r\cdot\boldsymbol{\sigma}_{ed}^*)(\boldsymbol{\sigma}_e\cdot\boldsymbol{\sigma}_{ed}^*)(\boldsymbol{\sigma}_r\cdot\boldsymbol{\sigma}_{ed}^{\perp *})M^2(k,d,\Delta n)\times \\ \times\left[1 - M^2(k,d,\Delta n)(\boldsymbol{\sigma}_r\cdot\boldsymbol{\sigma}_{ed}^*)^2R_dR_u\right]^{-1}\Big|^2,\end{aligned} \tag{12}$$

$$\begin{aligned}|R(d,L)^-|^2 = \\ = \Big|\{R_e^- + R_dT_eT_u^-M^2(k,d,\Delta n)(\boldsymbol{\sigma}_e\cdot\boldsymbol{\sigma}_{ed}^*)(\boldsymbol{\sigma}_r\cdot\boldsymbol{\sigma}_{ed}^{\perp *})\times \\ \times\left[1 - M^2(k,d,\Delta n)(\boldsymbol{\sigma}_r\cdot\boldsymbol{\sigma}_{ed}^*)^2R_dR_u\right]^{-1}\}\Big|^2,\end{aligned} \tag{13}$$

where R_e^- is the reflection coefficients of the CLC layer for light of nondiffracting circular polarization taking dielectric interfaces at the incidence of diffracting polarization light into account and T^- is the transmission coefficient of the CLC layer for light of nondiffracting circular polarization taking dielectric interfaces at the incidence of nondiffracting polarization light into account, and $\boldsymbol{\sigma}_{ed}^{\perp}$ is the polarization vector orthogonal to $\boldsymbol{\sigma}_{ed}$. We note that the amplitude transmission coefficients T_d^- and T_u^- are approximately equal to $\exp[ikLn_-/n_0]$, where n_- is the refractive index of light of the nondiffracting circular polarization in CLC layer.

Calculations of the reflection and transmission coefficients according to (9), (10), (12), and (13) can be performed analytically in the general case, but are rather cumbersome. This is why we study the case of low birefringence in detail below and present expressions for $|T(d,L)|^2$ and $|R(d,L)|^2$ taking only the polarization transformation in the defect layer into account and neglecting transformations of polarizations at the interfaces and small deviations of the diffracting and nondiffracting polarizations from the circular ones, which allows simple analytic calculations.

With these simplifications and under the assumption that the refractive indices of the DMS external media coincide with the average CLC refractive index, the refractive indices of the defect layer can be expressed by the formulas

$$n_{max} = n_0 + \Delta n/2, \quad n_{min} = n_0 - \Delta n/2, \tag{14}$$

where n_0 coincides with the average CLC refractive index and Δn is small. The phase factor $M(k,d,\Delta n)$ is given by

$$M(k,d,\Delta n) = \exp[ikd]\cos(\Delta\varphi/2), \tag{15}$$

where the phase difference of two beam components with different eigenpolarization at the defect layer thickness is $\Delta\varphi = \Delta nkd/n_0$, $k = \omega n_0/c = \omega\varepsilon_0^{1/2}/c$.

Finally, in the case of low birefringence, inserting (15) into (9) and (10), we obtain explicit expressions for the reflection and transmission coefficients of light with a circular diffracting polarization for the incident beam with a circular diffracting polarization:

$$|T(d,L)|^2 = \left|\frac{T_eT_d\exp[ikd]\cos(\Delta\varphi/2)}{1-\exp[2ikd]\cos^2(\Delta\varphi/2)R_dR_u}\right|^2, \tag{16}$$

$$\begin{aligned}|R(d,L)|^2 = \\ = \left|R_e + \frac{R_dT_eT_u\exp[2ikd]\cos^2(\Delta\varphi/2)}{1-\exp[2ikd]\cos^2(\Delta\varphi/2)R_dR_u}\right|^2.\end{aligned} \tag{17}$$

If $\Delta\varphi/2\pi$ is an integer, Eqs. (16) and (17) are identical to the corresponding equations for the DMS with an isotropic defect layer [12, 13] and there is no conversion of the diffracting polarization into a nondiffracting one, but if $\Delta\varphi/2\pi$ is not an integer, this conversion occurs and, consequently, light leaks from the DMS and, in particular, the DM lifetime is less than in the case of the corresponding DMS with an isotropic defect layer. This dependence of the DM properties on the phase shift between eigenwaves at their crossing the defect layer opens up the way to control the DM properties.

The simplest such possibility is related to variations of the defect layer thickness.

The polarization conversion results in adding the nondiffracting components to the transmitted and reflected beams. For low birefringence, which corresponds to the condition $\Delta n/n_0 < \delta$, the amplitude transmission and reflection coefficient for nondiffracting polarization light (for the incident light of diffracting polarization) are given by

$$T(d,L)^- = T_e \exp\frac{ikLn_-}{n_0} \times \\ \times \frac{\exp[ikd]\sin(\Delta\varphi/2)}{1-\exp[2ikd]\cos^2(\Delta\varphi/2)R_dR_u}, \quad (18)$$

$$R(d,L)^- = \frac{1}{2}R_uT_e \exp\frac{ikLn_-}{n_0} \times \\ \times \frac{\exp[2ikd]\sin(\Delta\varphi)}{1-\exp[2ikd]\cos^2(\Delta nkd/2n_0)R_dR_u}, \quad (19)$$

where n_- is the refractive index of light of nondiffracting circular polarization in the CLC layer.

The calculations results for the transmission $|T(d,L)|^2$ coefficient of light of diffracting polarization in the case of low birefringence are presented at Fig. 7 for various values of the birefringent phase factor $\Delta\varphi$ related to the light single propagation in a birefringent defect layer. Figure 7 shows that at low values of the phase shift between eigenwaves at their crossing the defect layer ($\Delta\varphi < \pi/2$), the shape of the transmission curve is very similar to that for a DMS with an isotropic defect layer (for $\Delta\varphi$ equal to an integer multiple of 2π or zero, it coincides with the shape of the corresponding curve for an isotropic defect layer). But as $\Delta\varphi$ approaches $\pi/2$ (see Fig. 7*e–g*), the increase in transmission at the defect mode frequency, typical for an isotropic defect layer, gradually disappears and does not appear at all at $\Delta\varphi = \pi/2$ (Fig. 7*g*). This may be regarded, in particular, as a hint that the DM lifetime decreases with increasing the shift between eigenwaves at their crossing the defect layer and that the DM does not exist at all at some value of the shift.

With the partial conversion of the circular nondiffracting incident polarization into the diffracting one taken into account, the picture of transmission spectra does not change radically. In Fig. 8, the transmission spectra for the total light intensity crossing the DMS (for the sum of intensities for both circular polarizations) calculated using Eqs. (18) and (19) show a general decrease in transmission at the DM frequency ω_D as $\Delta\varphi$ increases, but it is much more slow than for the diffracting polarization and only at $\Delta\varphi$ close to $\pi/2$ does the transmission practically vanish (which demonstrates the conversion of polarizations at the birefringent layer).

It is well known [9] that the position of the edge mode frequency in the stop-band is determined by the frequency of the transmission (reflection) coefficient maximum (minimum), and therefore the performed calculation of the transmission spectra (Figs. 7 and 8) determine the real component of the DM frequency. But because the DM is a quasistationary mode, the imaginary component of the DM frequency is not zero [12, 13]. A direct way to find the imaginary component of the DM frequency is to solve the dispersion equation. The dispersion equation in the case of a birefringent defect layer can be found similarly to the case of an isotropic defect layer [12, 13] and if multiple scattering of light of nondiffracting polarization is neglected, it can be represented as

$$M^2(k,d,\Delta n)\sin^2(qL) - \frac{\exp(-i\tau L)}{\delta^2}\left[\frac{\tau q}{\kappa^2}\cos(qL) + \\ + i\left(\left(\frac{\tau}{2\kappa}\right)^2 + \left(\frac{q}{\kappa}\right)^2 - 1\right)\sin(qL)\right]^2 = 0. \quad (20)$$

In the general case, the solution of Eq. (20) has to be found numerically, and a detailed discussion of this in the case of an isotropic defect layer can be found in [12, 13]. Some simplification of (20) occurs in the case of low birefringence, when the phase factor in (20) is given by (15).

3.2. Amplifying and absorbing CLC layers

As the experiment [3] and the theory [12, 13] show, unusual optical properties of the DMS at the DM frequency ω_D (abnormally strong absorption for an absorbing CLC and abnormally strong amplification for an amplifying CLC [12, 13, 25, 30]) can be effectively used for enhancing DFB lasing. It is quite natural to study how the birefringent defect layer influences the abnormally strong amplification and abnormally strong absorption effects. For studying this, we assume, as was done in [12, 13], that the average dielectric constant of the CLC has an imaginary addition, i. e., $\varepsilon = \varepsilon_0(1+i\gamma)$, where positive γ corresponds to absorbing and negative γ to amplifying media. (We note that in real situations, $|\gamma| \ll 1$.) As was mentioned above, the value of γ can be found from solution of dispersion equation (20). Another option (see [12, 13]) is to study reflection and transmission coefficients (9), (10), (16), (17) as functions of γ close to $R(d,L)$ and $T(d,L)$ at the DM frequency.

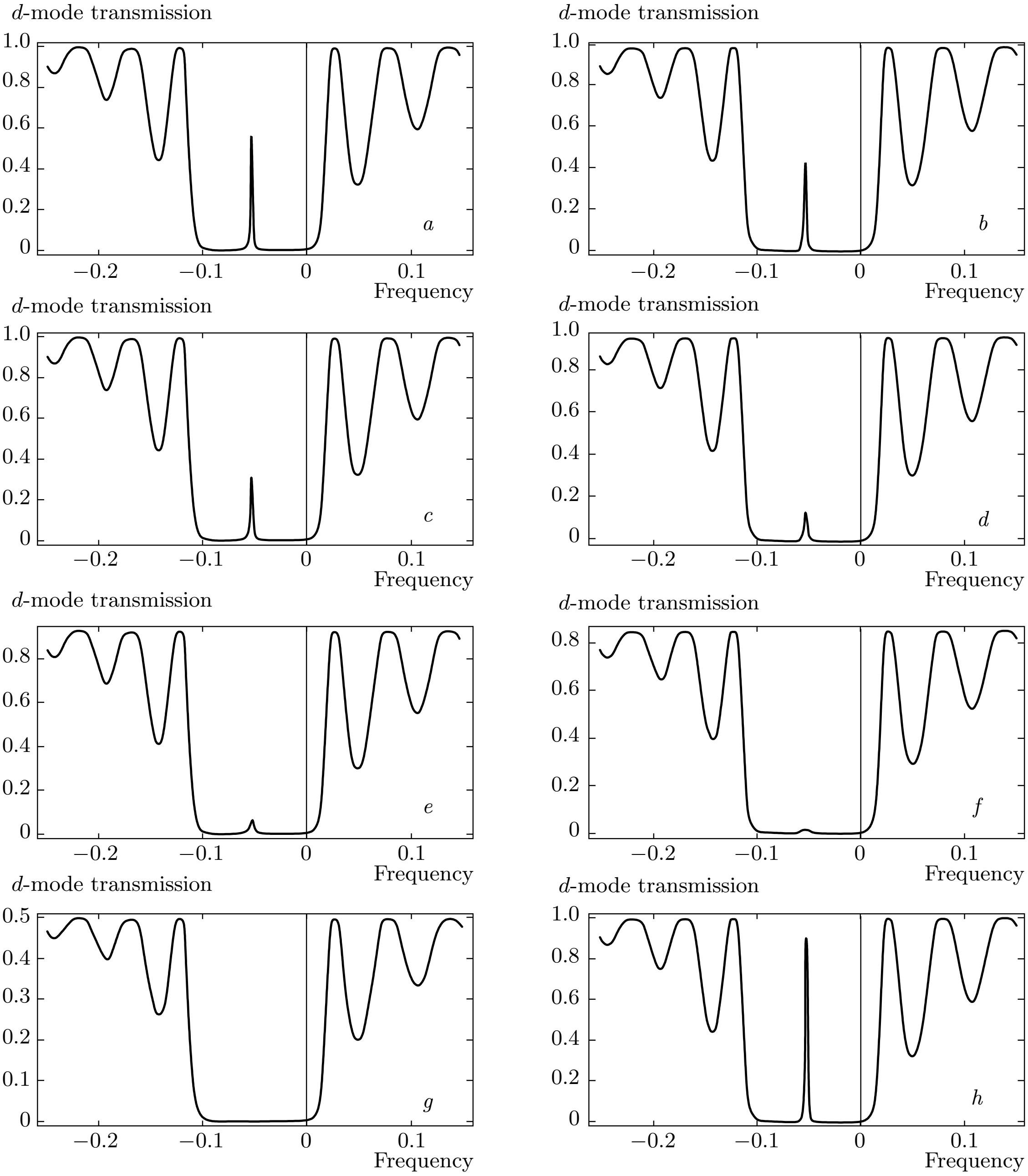

Fig. 7. The calculated diffracting polarization intensity transmission coefficient $|T(d,L)|^2$ for a low-birefringent defect layer versus the frequency for a diffracting incident polarization at the birefringent phase shift at the defect layer thickness $\Delta\varphi = \pi/20$ (a), $\pi/16$ (b), $\pi/12$ (c), $\pi/8$ (d), $\pi/6$ (e), $\pi/4$ (f), $\pi/2$ (g), and $\Delta\varphi = 0$ (h) (Fig. 7h corresponds to the isotropic defect layer) for a nonabsorbing CLC at $d/p = 0.25$

For an amplifying CLC, the value of γ corresponding to a divergence of the DMS reflection and transmission coefficients just determines the solution of dispersion equation (20) and also determines the threshold DFB lasing gain in the DMS (see [12, 13]). Therefore the threshold value of γ can be found by calculating the DMS reflection and transmission coefficients at various γ and finding its value at the points where the DMS reflection and transmission coefficients diverge.

This procedure, performed here for a birefringent defect layer at various values of the birefringent phase factor $\Delta\varphi$ related to the light single propagation in a birefringent defect layer, allows tracing the threshold lasing gain (γ) dependence on the birefringent phase

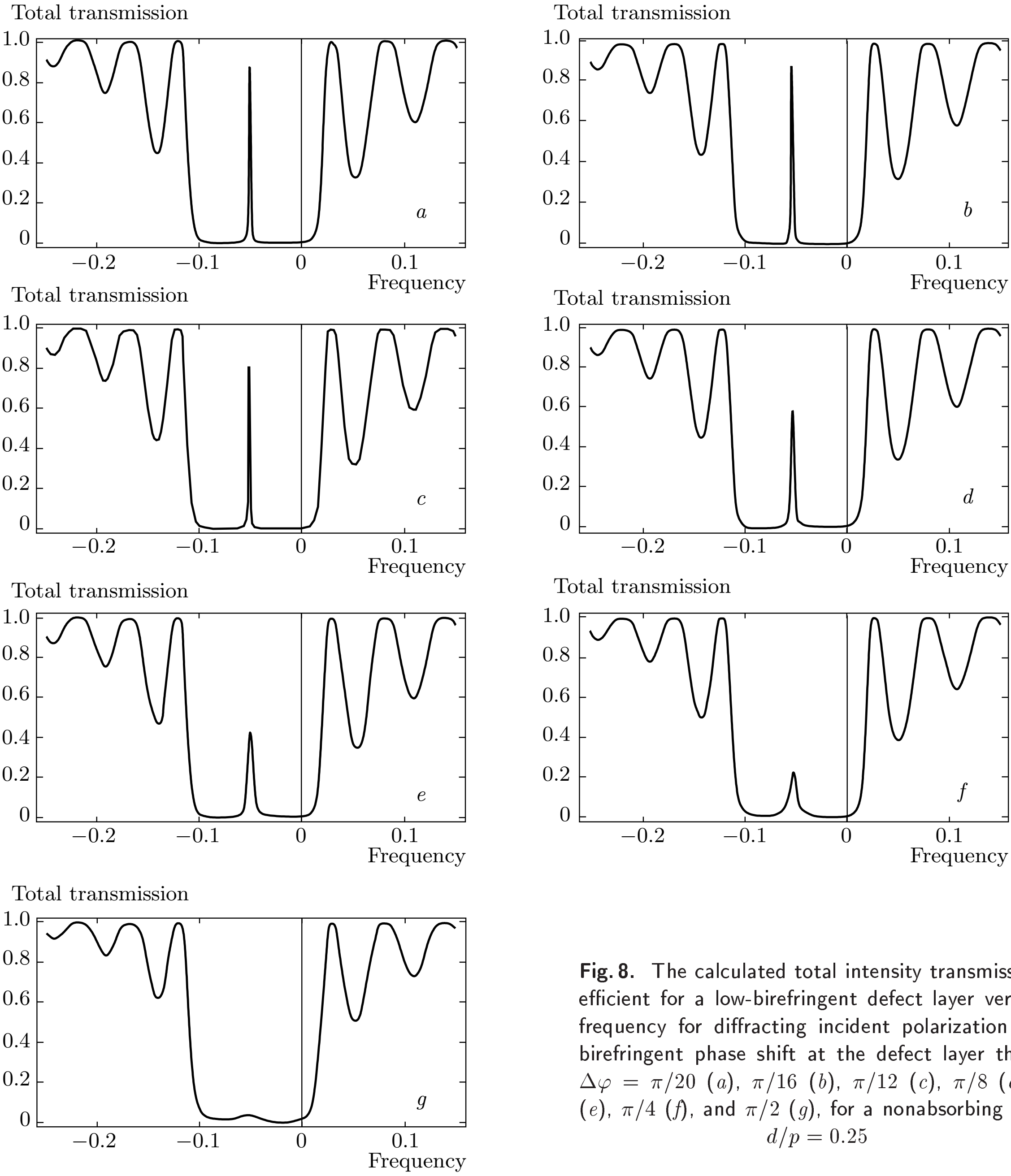

Fig. 8. The calculated total intensity transmission coefficient for a low-birefringent defect layer versus the frequency for diffracting incident polarization at the birefringent phase shift at the defect layer thickness $\Delta\varphi = \pi/20$ (*a*), $\pi/16$ (*b*), $\pi/12$ (*c*), $\pi/8$ (*d*), $\pi/6$ (*e*), $\pi/4$ (*f*), and $\pi/2$ (*g*), for a nonabsorbing CLC at $d/p = 0.25$

factor $\Delta\varphi$. Figure 9, presenting the values of the DMS transmission coefficient close to their divergence points, demonstrates increase in the threshold DFB lasing gain ($|\gamma|$) with an increase in the birefringent phase factor $\Delta\varphi$ and even the disappearance of the divergence at the DM frequency at $\Delta\varphi = \pi/2$. This is in good agreement with the transmission spectra calculated in Figs. 7 and 8. In particular, at $\Delta\varphi = \pi/2$, there are no traces of the typical DM peculiarities in transmission spectra.

For absorbing CLC layers in the DMS, the abnormally strong absorption effect reveals itself at the value of γ ensuring a maximum of the total absorption in the DMS (see [12, 13]). For a finite thickness L of CLC layers, the DM frequency ω_D is a complex quantity, which can be found by a numerical solution of Eq. (20). As in the case of absorbing and amplifying defect layers, the positions of dips in reflection and spikes in transmission inside the stop-band just correspond to $\operatorname{Re}\omega_D$,

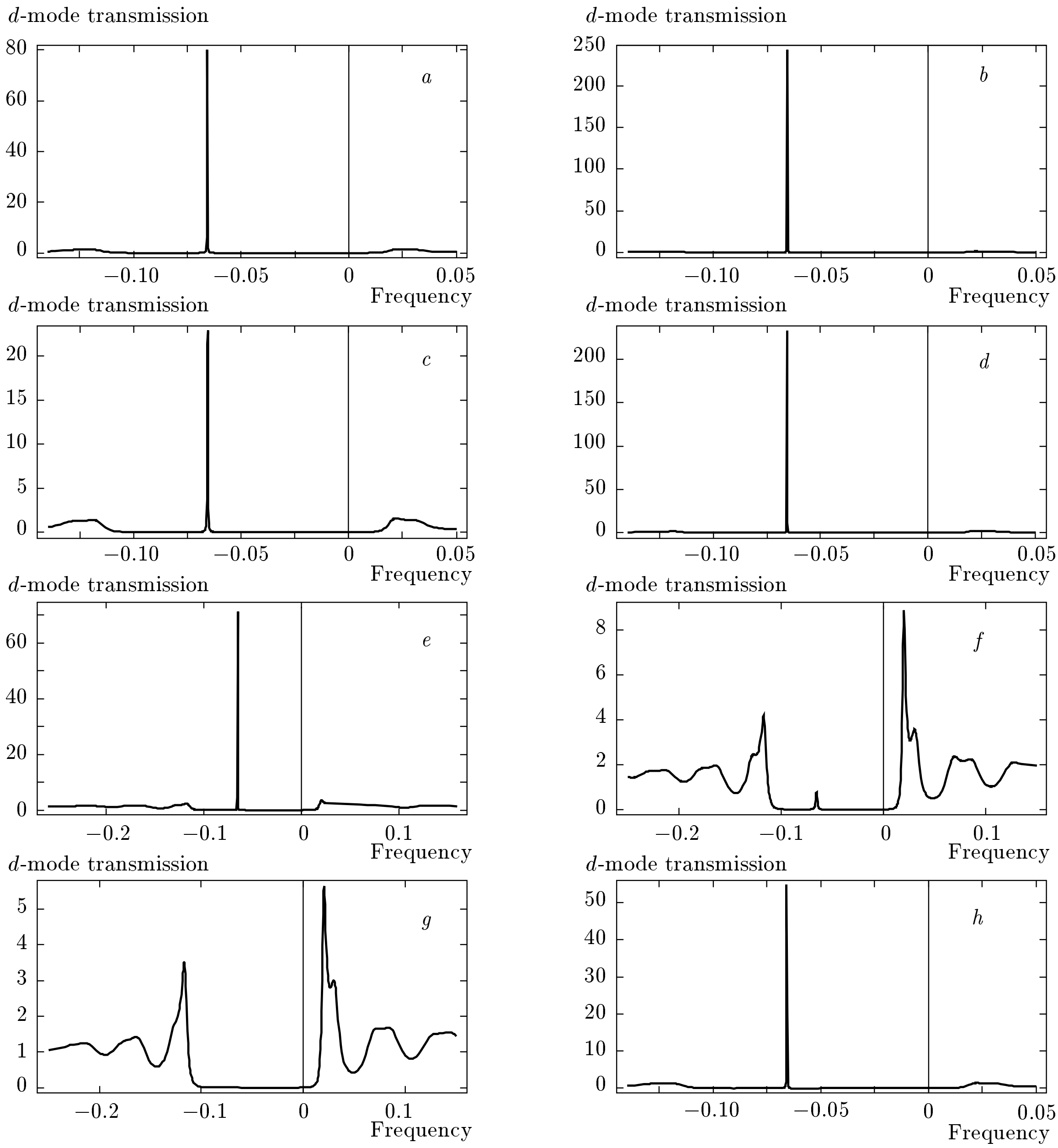

Fig. 9. The calculated intensity transmission coefficients of a low-birefringent defect layer for an amplifying CLC layers versus the frequency close to their divergence points as a function of γ for diffracting incident polarization at the birefringent phase shift at the defect layer thickness $\Delta\varphi = \pi/20$ (a), $\pi/16$ (b), $\pi/12$ (c), $\pi/8$ (d), $\pi/6$ (e), $\pi/4$ (f), and $\pi/2$ (g); $\gamma = -0.00075$ (a), -0.00085 (b), -0.00100 (c), -0.00150 (d), -0.002355 (e), -0.003555 (f), -0.004500 (g), and $\Delta\varphi = 0$, $\gamma = -0.000675$ (h) corresponding to an isotropic defect layer; $d/p = 2.25$

and this observation turns out to be useful for numerically solving the dispersion equation for a birefringent defect layer and absorbing CLC layers.

We note that the results obtained here for the DMS with a birefringent defect layer open up new options for varying the DM characteristics. An important result related to DFB lasing at the DMS with a birefringent defect layer can be formulated as follows. The lasing threshold gain increases with an increase in the optical path difference of two eigenwaves at the defect layer thickness. A similar result relates to the effect of anomalously strong absorption, where the value of maximal absorption is dependent on the optical path difference at the defect layer thickness.

4. DEFECT STRUCTURE WITH A DIELECRIC JUMP

An isotropic defect layer with the dielectric constant differing from the average dielectric constant ε_0 of CLC layers can also be effectively related to the case of an active defect layer. The reason for this is the polarization conversion at the defect layer surfaces, which makes this case similar to the case of a birefringent defect layer. If the dielectric constant of the medium external to the DMS is different from the average dielectric constant ε_0 of CLC layers, polarization conversion also occurs at the external DMS surfaces, but, as we see below, the polarization conversion at the external DMS surfaces does not affect the DM properties so strong as the polarization conversion at the defect layer surfaces does. There are no principal difficulties in obtaining the DM dispersion equation from the boundary conditions in the general case of dielectric jumps at all interfaces of the DMS. But the DM dispersion equation is rather complicated in the general case (a system of 12 linear equations). Therefore, we first demonstrate the role of dielectric jumps for a localized mode in the simplest case of an edge mode (EM), which is related to a CLC layer with dielectric jumps at its surfaces.

4.1. Dielectric jumps at a single CLC layer

In accordance with the foregoing, we study the transmission and reflection of light by a CLC layer surrounded by a medium with the dielectric constant differing from the average CLC dielectric constant ε_0 for light propagation along the helical axis (see the schematic of the boundary value problem in Fig. 10). Following the approach in [25, 26, 31], from the boundary conditions, we obtain the system of equations for

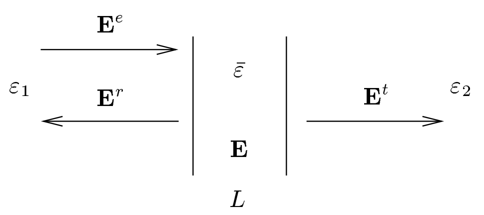

Fig. 10. Schematic of the CLC edge mode structure with dielectric jumps at the interfaces

the amplitudes E_j^+ of eigenwaves in the layer excited by an external wave incident at the layer:

$$
\begin{aligned}
&\sum_{j=1}^{4}\left(1+\frac{K_j^+}{\kappa_{e,1}}\right)E_j^+ = 2E_e^+,\\
&\sum_{j=1}^{4}\exp(iK_j^+L)\left(1-\frac{K_j^+}{\kappa_{e,2}}\right)E_j^+ = 0,\\
&\sum_{j=1}^{4}\xi_j\left(1+\frac{K_j^-}{\kappa_{e,1}}\right)E_j^+ = 2E_e^-,\\
&\sum_{j=1}^{4}\xi_j\exp(iK_j^-L)\left(1-\frac{K_j^-}{\kappa_{e,2}}\right)E_j^+ = 0,
\end{aligned}
\tag{21}
$$

where the incident, reflected, and transmitted waves and the wave inside the CLC are written as follows:

$$
\begin{aligned}
\mathbf{E}^e &= \exp\left[i(\kappa_{e,1}z-\omega t)\right]\left(E_e^+\mathbf{n}_+ + E_e^-\mathbf{n}_-\right),\\
\mathbf{E}^r &= \exp\left[-i(\kappa_{e,1}z-\omega t)\right]\left(E_r^+\mathbf{n}_- + E_r^-\mathbf{n}_+\right),\\
\mathbf{E}^t &= \exp\left[i(\kappa_{e,2}z-\omega t)\right]\left(E_t^+\mathbf{n}_+ + E_t^-\mathbf{n}_-\right),
\end{aligned}
$$

$$
\mathbf{E} = \exp(-i\omega t)\times \\
\times\sum_{j=1}^{4}E_j^+\left(\exp(iK_j^+z)\mathbf{n}_+ + \xi_j\exp(iK_j^-z)\mathbf{n}_-\right),
$$

with $\mathbf{n}_\pm$ being the left and right circular polarization vectors (see Eq. (11)); we here use the labeling of CLC eigenwaves proposed in [25, 26, 31] (the subscripts "1" and "4" correspond to nondiffracting eigenwaves propagating in the opposite directions and the subscripts "2" and "3" correspond to diffracting eigenwaves).

The wave vectors inside the CLC layer are

$$
K_1^+ = \tau/2+q_+,\quad K_4^+ = \tau/2-q_+,
$$

$$
q_+ = \kappa\left\{1+(\tau/2\kappa)^2+\left[(\tau/\kappa)^2+\delta^2\right]^{1/2}\right\}^{1/2},
$$

$$
K_2^+ = \tau/2+q,\quad K_3^+ = \tau/2-q,
$$

and q is determined by Eq. (4),

$$
K_j^- = K_j^+-\tau,\quad \kappa_{e,1} = \frac{\omega\sqrt{\varepsilon_1}}{c},\quad \kappa = \frac{\omega\varepsilon_0^{1/2}}{c},
$$

$$
\kappa_{e,2} = \frac{\omega\sqrt{\varepsilon_2}}{c},\quad \xi_i = \frac{\delta}{(K_j^+/\kappa-\tau/\kappa)^2-1}.
$$

The amplitudes of reflected and transmitted waves are expressed in terms of $E_j^\pm$:

$$
\begin{aligned}
E_r^+ &= \frac{1}{2}\sum_{j=1}^{4}\xi_j\left(1-\frac{K_j^-}{\kappa_{e,1}}\right)E_j^+,\\
E_t^+ &= \frac{1}{2}\sum_{j=1}^{4}\exp\left[i(K_j^+-\kappa_{e,2})L\right]\times\\
&\qquad\qquad\times\left(1+\frac{K_j^+}{\kappa_{e,2}}\right)E_j^+,\\
E_r^- &= \frac{1}{2}\sum_{j=1}^{4}\left(1-\frac{K_j^+}{\kappa_{e,1}}\right)E_j^+,\\
E_t^- &= \frac{1}{2}\sum_{j=1}^{4}\xi_j\exp\left[i(K_j^--\kappa_{e,2})L\right]\times\\
&\qquad\qquad\times\left(1+\frac{K_j^-}{\kappa_{e,2}}\right)E_j^+.
\end{aligned}
\tag{22}
$$

It is convenient to introduce the parameters $r_1 = \varepsilon_0^{1/2}/\varepsilon_1^{1/2} = k/k_{e,1}$ and $r_2 = \varepsilon_0^{1/2}/\varepsilon_2^{1/2} = k/k_{e,2}$, reducing the ratios $K_j^{\pm}/k_{e,i}$ in Eqs. (21) and (22) to the $r_i K_j^{\pm}/k$. For the sake of generality, the case of different dielectric constants of the media surrounding the CLC layer is shown in Fig. 10 and, accordingly, Eqs. (21) and (22) relate to the case of different media at the sides of the CLC layer.

Examples of calculations performed with (21) and (22), which demonstrate the influence of dielectric jumps at the layer surfaces on the transmission and reflection coefficients, are presented in [32]. Here, we do not discuss the transmission and reflection of light by a layer but concentrate on the influence of dielectric jumps at the layer surfaces on the EM properties. The EMs are determined by the homogeneous system corresponding to system (21) and the EM dispersion equation for the EM frequency follows from the solvability condition for this homogeneous system [33]. It is known [33] that the real part of the EM frequency approximately coincides with the frequency positions of reflection coefficient minima, and hence the solution of the homogeneous system at the frequency of the reflection coefficient minimum gives the amplitudes of all four eigenwaves in the layer composing the EM in the case where the dielectric constants of the media surrounding the CLC layer are different from ε_0. We recall that the EM in the absence of dielectric constant jumps at the interfaces is composed only from two diffracting eigenwaves [33]. Because of a sufficiently cumbersome form of the homogeneous system solution, we first use the consecutive approximation approach in solving the system. If the layer thickness is sufficiently large, the known solution [33] in the absence of dielectric constant jumps can be used as the zeroth approximation. In this approximation, the homogeneous system under consideration reduces to a system of two equations for the amplitudes of two nondiffracting eigenwaves E_1^+ and E_4^+. The solution of the homogeneous system thus found at the EM frequency shows that the amplitude of two nondiffracting eigenwaves in the solution for the EM decrease inversely proportionally to the layer thickness L. This result shows that if the CLC layer thickness is large enough, the influence of the dielectric constant jumps at the layer surfaces is small and in the limit of an infinitely thick CLC layer, the EM properties are the same as in the absence of dielectric constant jumps. In Fig. 11*a*, the calculated variations of the EM lifetime versus the layer thickness L are presented in the case where dielectric jumps are absent and for two values of the dielectric jump (in Fig. 11*b*, a small part of the curve in Fig. 11*a* is presented in an enlarged scale). The calculations of the EM lifetime versus the layer thickness L presented in Fig. 11 confirm the above statement showing that as L increases, the EM lifetime ($\operatorname{Im}\omega$), with decaying oscillations, approaches the value corresponding to the absence of dielectric jumps.

4.2. Dielectric jumps at the defect layer

We return to the case of a DMS with an isotropic defect layer and with the dielectric constant differing from the average dielectric constant ε_0 of CLC layers. In the general case of dielectric jumps at all interfaces in the DMS (see Fig. 1), we have to determine 12 amplitudes of eigenwaves propagating in the DMS (four amplitudes in each CLC layer and four amplitudes for waves propagating in the isotropic defect layer in both directions for the opposite circular polarizations). To simplify the problem, we assume that there are no dielectric jumps at the external DMS surfaces. As we have seen, the dielectric jumps at external DMS surfaces for thick CLC layers do not significantly affect the polarization conversion. We therefore take the dielectric jumps into account only at the interfaces with defect layer. Taking the form of the DM solution in the absence of dielectric jumps into account [12, 13], we have to determine only eight amplitudes of eigenwaves propagating in the DMS (two amplitudes in each CLC layer and four amplitudes for waves propagating in the isotropic defect layer).

If we accept the labeling of eigenwaves in the CLC proposed in [25, 26, 31] and specify them by superscripts "u" and "d" for the upper and bottom CLC layers in Fig. 1, then the corresponding system includes E_2^u, E_4^u, E_1^d, and E_2^d, the amplitudes of eigenwaves in the CLC, and $C_R^{\pm}$ and $C_L^{\pm}$, the amplitudes of right (left)

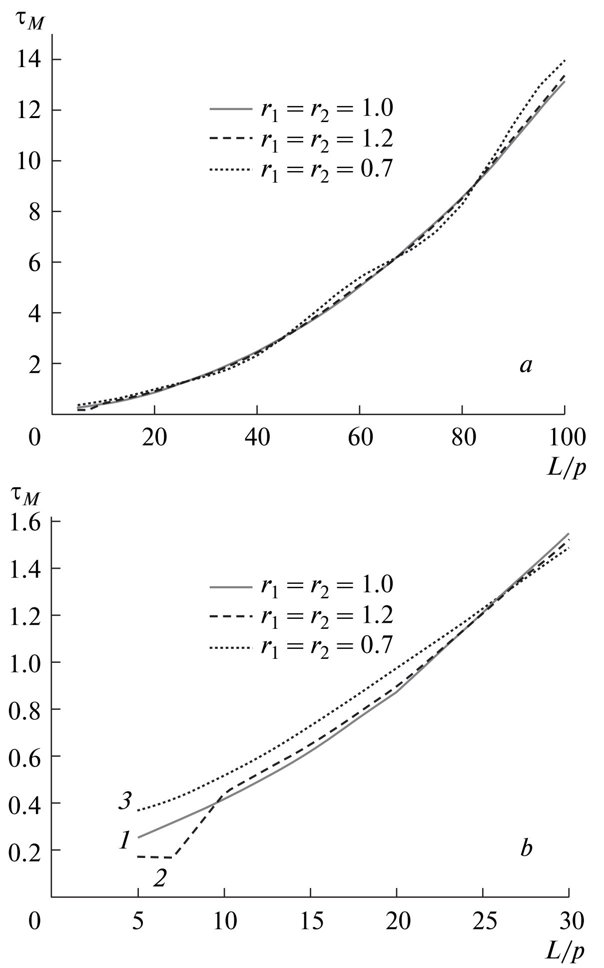

Fig. 11. a) The calculated EM lifetime versus the CLC layer thickness normalized by the CLC layer flight time $\varepsilon_0^{1/2}L/c$ for several values of the dielectric jump at the CLC layer surface, b) magnified part of Fig. 11a

polarized waves in the defect layer with two ($\pm$) possible propagation directions. We assume for definiteness that the diffracting circular polarization is the right-hand one. If we accept the following ordering E_2^u, E_4^u, C_R^+, C_R^-, C_L^+, C_L^-, E_1^d, E_2^d of the amplitudes in the equations obtained from the boundary conditions, then the elements of the matrix a_{ik} of the corresponding system of equations are as follows:

$$a_{ik} = 0 \quad \text{for} \quad i = 5,6,7,8 \quad \text{and} \quad k = 1,2;$$

$$a_{ik} = 0 \quad \text{for} \quad i = 1,2,3,4 \quad \text{and} \quad k = 7,8;$$

$$a_{11} = \exp(iK_2^+L_-) - \exp(iK_3^+L_-),$$

$$a_{12} = \exp(iK_4^+L_-), \quad a_{13} = \exp(ik_dL_-),$$

$$a_{1k} = 0 \quad \text{for} \quad k = 4,5; \quad a_{16} = \exp(-ik_dL_-);$$

$$a_{21} = \zeta_2 \exp(iK_2^-L_-) - \zeta_3 \exp(iK_3^-L_-),$$

$$a_{22} = \zeta_4 \exp(-iK_4^-L_-), \quad a_{2k} = 0 \quad \text{for} \quad k = 3,6;$$

$$a_{24} = \exp(-ik_dL_-), \quad a_{25} = \exp(ik_dL_-);$$

$$a_{31} = -K_2^+ exp(iK_2^+L_-) - K_3^+ \exp(iK_3^+L_-),$$

$$a_{32} = -K_4^+ \exp(iK_4^+L_-), \quad a_{33} = -k_d \exp(ik_dL_-),$$

$$a_{3k} = 0 \quad \text{for} \quad k = 4,5; \quad a_{35} = k_d \exp(-ik_dL_-);$$

$$a_{41} = K_2^- \zeta_2 \exp(iK_2^-L_-) - \zeta_3 K_3^- \exp(iK_3^-L_-),$$

$$a_{42} = -\zeta_4 K_4^- \exp(-iK_4^-L_-),$$

$$a_{4k} = 0 \quad \text{for} \quad k = 3,6;$$

$$a_{44} = -k_d \exp(-ik_dL_-), \quad a_{45} = k_d \exp(ik_dL_-);$$

$$a_{53} = \exp(ik_dL_+), \quad a_{5k} = 0 \quad \text{for} \quad k = 4,5;$$

$$a_{56} = \exp(-ik_dL_+), \quad a_{57} = \exp(iK_1^+L_+),$$

$$a_{58} = \exp(iK_2^+L_+) - r_{32} \exp(iK_3^+L_+);$$

$$a_{6k} = 0 \quad \text{for} \quad k = 3,6;$$

$$a_{64} = \exp(-ik_dL_+), \quad a_{67} = \zeta_1 \exp(ik_dL_+),$$

$$a_{68} = \zeta_2 \exp(iK_2^-L_+) - r_{32}\zeta_3 \exp(iK_3^-L_+),$$

$$a_{74} = -k_d \exp(ik_dL_+), \quad a_{7k} = 0 \quad \text{for} \quad k = 4,5;$$

$$a_{77} = K_1^+ \exp(iK_1^+L_+),$$

$$a_{78} = -K_2^+ \exp(iK_2^+L_+) + r_{32}K_3^+ \exp(iK_3^+L_+);$$

$$a_{8k} = 0 \quad \text{for} \quad k = 3,6; \quad a_{84} = -k_d \exp(-ik_dL_+),$$

$$a_{85} = k_d \exp(ik_dL_+), \quad a_{87} = \zeta_1 K_1^- \exp(-iK_1^-L_+),$$

$$a_{88} = K_2^- \zeta_2 \exp(iK_2^-L_+) - r_{32}\zeta_3 K_3^- \exp(iK_3^-L_+),$$

where $r_{32} = (\zeta_2/\zeta_3)\exp(4iqL)$.

The dispersion equation for the DM frequency ω_D and, in particular, the DM lifetime ($\operatorname{Im}\omega_D$) for a DMS with dielectric jumps only at the interfaces with the defect layer is determined by the equation following from the zero value condition for the determinant of the above matrix. The corresponding equation requires a numerical approach for its solution. However, a simple estimate of the DM lifetime can be obtained.

As is known, the DM lifetime for a DMS with no dielectric jumps at the interfaces is determined by the leakage of energy through the external DMS surfaces [13] and the lifetime increases with the CLC layer thickness increase, being infinite for an infinite CLC layer thickness. The changes in the DM lifetime for a DMS with dielectric jumps at the interfaces compared to the case without jumps are mainly connected with the conversion of the diffracting polarization into the nondiffracting one and free escaping of light with nondiffracting polarization from the DMS. If the CLC layer thickness is large enough, this mechanism is prevailing over the leakage of light with the diffracting polarization through the external DMS surfaces. This is why if the CLC layer thickness in the DMS is sufficiently large, the DM lifetime is mainly determined by the polarization conversion at the interfaces with the defect layer. Hence, for estimating the DM lifetime for a DMS with dielectric jumps at the interfaces, we can use the formula for the DM lifetime due to the leakage of energy through the external DMS surfaces in the case of no dielectric jumps at the interfaces (formula (22) in [13]), with the amplitude of the wave with converted polarization at the defect layer surface inserted into it instead of the diffracting wave amplitude leaking through the DMS external surface. The amplitude of the wave with the converted polarization can be approximately found if, in the solving the homogeneous system, we assume that the field in the CLC layers is the same as for the DMS without dielectric jumps. This means that the amplitudes E_2^u, C_R^+, C_R^-, and E_2^d are the same as for the EM in a DMS without dielectric jumps and $E_1^d = E_4^u = 0$; however, C_L^+ and C_L^- have to be found. We easily find the values of C_L^+ and C_L^- using expressions for the EM field from [13]. The next step is to express the nonzero E_1^d and E_4^u, which determine the field of nondiffracting circular polarization escaping from the DMS through the external surfaces, in terms of the known E_2^u, C_R^+, C_R^-, E_2^d and the found C_L^+ and C_L^-. A rather crude estimate can be obtained without finding E_1^d and E_4^u, by calculating the direct polarization conversion at the interface with the defect layer for light of diffracting polarization (for the DM field at the DMS without dielectric jumps). For such an estimate of polarization conversion, we can apply the formulas for polarization conversion at the interface of the CLC and an isotropic medium presented in [25, 26, 31]. The reflection coefficient of light of diffracting circular polarization into light of nondiffracting circular polarization at a semi-infinite CLC layer R^{+-} and the transmission coefficient of light of nondiffracting circular polarization for an incident light of diffracting circular polarization T^{+-} in the zeroth order in δ are given by

$$R^{+-} = \frac{(1-r)^2}{(1+r)^2}, \quad T^{+-} = \frac{4r(1-r)^2}{(1+r)^4}, \tag{23}$$

where $r = (\varepsilon_d/\varepsilon_0)^{1/2}$ and ε_d is the defect layer dielectric constant.

Because circular polarization conversion at the interface of CLC and the isotropic medium is proportional to the square of the small parameter δ even in the absence of dielectric jumps [25, 26, 31], polarization conversion at the interfaces should be taken into account if the dielectric jump is sufficiently large ($|r-1| > \delta$). Therefore, the accuracy of expressions (23) under these conditions is sufficient for estimating the influence of dielectric jumps on the DM lifetime in this case. The results of the corresponding analysis are as follows. The DM lifetime for a DMS with dielectric jumps at the interfaces increases with an increase in the CLC layer thickness to the value for which the leakage of energy through the external surfaces and the leakage due to the conversion of diffracting polarization light into light of nondiffracting polarization become approximately equal. At a further increase in the CLC layer thickness, the DM lifetime is determined almost exclusively by the polarization conversion at the defect layer surfaces and becomes practically independent of the CLC layer thickness L or, more correctly, becomes a very slowly increasing function of L. If, following [13], we represent the DM lifetime for the DMS with dielectric jumps at the interfaces τ_{dr} as the ratio of the optical field energy in the DMS to the energy flow of light of converted polarization through the defect layer surfaces, then the relation of τ_{dr} to the DM lifetime τ_d for a DMS without dielectric jumps at the interfaces can be estimated as

$$\tau_{dr} = \frac{\varepsilon_0^{1/2}}{c} \int \frac{|E(\omega_D, z, t)|^2 dz}{2r(1-r)^2|E_{dr}|^2/(1+r)^4} = \\ = \frac{\tau_d |E^{out}|^2}{2r(1-r)^2|E_{dr}^u|^2/(1+r)^4}, \tag{24}$$

where r is defined in (23) and all other quantities in (24) are related to the DM at the DMS without dielectric jumps: $E(\omega_D, z, t)$ is the EM field in the CLC layer, E_{dr} is the DM field at the defect layer surface of light propagating toward the CLC layer as a function of the coordinate z along the layer normal and the time t, E^{out} is the EM field of light propagating outward the CLC layer at the external CLC layer surface, ω_D is the DM frequency, and the integration over z is carried out over the thickness L of CLC layer. Equation (24) shows that the DM lifetime for a DMS with thick CLC layers and dielectric jumps at the interfaces τ_{dr}, in contrast to the lifetime τ_d of a DM in the DMS without dielectric jumps at the interfaces, does not increase exponentially with L. The exponential increase of τ_d is compensated in Eq. (24) by the exponential increase of $|E_{dr}^u|^2$ (see [13]). For the restoration of the τ_{dr} exponential increase with L, the sharp jumps of the dielectric constant should be substituted by a smooth variation of the dielectric constant at defect layer surfaces. We note that sharp jumps at the interfaces have a negative effect on the possibility of lowering the lasing threshold, and therefore smoothing the dielectric jumps opens up options for lowering the lasing threshold compared with the case of the DMS with jump-like variations of the dielectric parameters.

In general, the localized optical modes in chiral liquid crystals theoretically studied in this section for a structure with jumps of the dielectric properties at their interfaces reveal a significant influence of the dielectric jumps on the EM and especially DM properties, in particular, its lifetime. The studied effects pave the way to optimizing the DM parameters by means of a proper choice of the defect layer dielectric properties.

5. CONCLUSION

As we have seen, isotropic defect layers with dielectric properties differing from those of the CLC layers in the DMS can be effectively regarded as active defect layers. Our analytic description of the defect modes at active defect layers (amplifying (absorbing), birefringent, and with dielectric jumps) allows revealing a clear physical picture of these modes, which is applicable to the defect modes in general (see [34]). For example, a lower lasing threshold and stronger absorption (under the conditions of the anomalously strong absorption effect) at the defect mode frequency at the middle of stop-band, compared to the defect mode frequency close to the stop-band edge, are the features of any periodic media. The obtained results demonstrate numerous possibilities to influence the DM properties by varying the defect layer dielectric characteristics. For a special choice of the parameters in the experiment, the obtained formulas can be directly applied to the experiment. Some results allow obtaining a qualitative explanation of the observed effects. This relates, for example, to the experimentally observed [3] circular polarization sense of the wave emitted from the defect structure above the lasing threshold, which is opposite to the polarization sense responsible for the defect mode existence. An obvious explanation of the "lasing" at the opposite (nondiffracting) circular polarization is as follows. Due to the polarization conversion of the generated wave into a wave of the opposite circular polarization, the converted wave of a nondiffracting polarization freely escapes from the structure. As was mentioned above, this polarization conversion phenomenon due to both birefringence and dielectric jumps also makes a contribution to the frequency width of the defect mode. However, in the general case, a quantitative description of the measurements reqiures taking all possible "active properties" of the defect layer into account using the above formulas.

We note that the obtained results for the DM at the DMS consisting of CLC layers are qualitatively applicable to the corresponding localized electromagnetic modes in any periodic media and can be regarded as a useful guide in the studies of localized modes with an active defect layer in general.

The work was supported by the RFBR (grants №№ 12-02-01016-a, 14-02-92601-RS-a, and 14-02-90008-Bel-a).

REFERENCES

1. Y.-C. Yang, C.-S. Kee, J.-E. Kim et al., Phys. Rev. E **60**, 6852 (1999).

2. V. I. Kopp and A. Z. Genack, Phys. Rev. Lett. **89**, 033901 (2003).

3. J. Schmidtke, W. Stille, and H. Finkelmann, Phys. Rev. Lett. **90**, 083902 (2003).

4. P. V. Shibaev, V. I. Kopp, and A. Z. Genack, J. Phys. Chem. B **107**, 6961 (2003).

5. M. A. Matranga, M. P. DeSanto, G. Petriashvili, A. Chanishvili, G. Chilaya, and R. Barbery, Ferroelectrics **395**, 1 (2010).

6. H. Yoshida, C. H. Lee, Y. Miura, A. Fujii, and M. Ozaki, Thin Solid Films **516**, 2358 (2008).

7. Y. Takanishi, Y. Ohtsuka, G. Suzaki, S. Nashimura, and H. Takezoe, Opt. Express **18**, 12909 (2010).

8. A. V. Shabanov, S. Ya. Vetrov, and A. Yu. Karneev, Pis'ma v Zh. Eksp. Teor. Fiz. **80**, 206 (2004) [JETP Lett. **80**, 181 (2004)].

9. V. I. Kopp, Z.-Q. Zhang, and A. Z. Genack, Prog. Quant. Electron. **27**(6), 369 (2003).

10. M. Becchi, S. Ponti, J. A. Reyes, and C. Oldano, Phys. Rev. B **70**, 033103 (2004).

11. J. Schmidtke and W. Stille, Europ. Phys. J. **90**, 353 (2003).

12. V. A. Belyakov, MCLC **494**, 127 (2008).

13. V. A. Belyakov and S. V. Semenov, Zh. Eksp. Teor. Fiz. **139**, 798 (2011) [JETP **112**, 694 (2011)].

14. V. A. Belyakov, MCLC **559**, 39 (2012).

15. V. A. Belyakov, MCLC **559**, 50 (2012).

16. E. Yablonovitch, T. J. Gmitter, R. D. Meade et al., Phys. Rev. Lett. **67**, 3380 (1991).

17. V. G. Arkhipkin, V. A. Gunyakov, S. A. Myslivets et al., Zh. Eksp. Teor. Fiz. **139**, 666 (2011).

18. I. J. Hodkinson, Q. H. Wu, K. E. Thorn, A. Lakhtakia, and W. McCall, Opt. Comm. **184**, 57 (2000).

19. F. Wang and A. Lakhtakia, Opt. Express **13**, 7319 (2005).

20. M. H. Song, N. Y. Ha, K. Amemiya et al., Adv. Mater. **18**, 193 (2006).

21. H. Yoshida, C. H. Lee, A. Fuji, and M. Ozaki, Appl. Phys. Lett. **89**, 231913 (2006).

22. H. Yoshida, R. Ozaki, K. Yoshino, and M. Ozaki, Thin Solid Films **509**, 197 (2006).

23. A. H. Gevorgyan and M. Z. Haratyunyan, Phys. Rev. E **76**, 031701 (2007).

24. M. H. Song, B. Park, Y. Takanishi et al., Jpn. J. Appl. Phys. **44**, 8165 (2005).

25. V. A. Belyakov and V. E. Dmitrienko, *Optics of Chiral Liquid Crystals*, in *Soviet Scientific Reviews*, Sect. A, Physics Reviews, ed. by I. M. Khalatnikov, Harwood Acad. Publ., London (1989), Vol. 13, p. 54.

26. V. A. Belyakov, *Diffraction Optics of Complex Structured Periodic Media*, Springer-Verlag, New York (1992), ch. 4.

27. H. de Vries, Acta Cryst. **4**, 219 (1951).

28. E. I. Kats, Zh. Eksp. Teor. Fiz. **33**, 634 (1971) [Sov. Phys. JETP **32**, 1004 (1971)].

29. P. G. de Gennes and J. Prost, *The Physics of Liquid Crystals*, Clarendon Press, Oxford (1993).

30. V. A. Belyakov, A. A. Gevorgian, O. S. Eritsian, and N. V. Shipov, Zh. Tekhn. Fiz. **57**, 1418 (1987) [Sov. Phys. Techn. Phys. **32**, 843 (1987)]; Sov. Phys. Crystalogr. **33**, 337 (1988).

31. V. A. Belyakov and A. S. Sonin, *Optika Kholestericheskih Zhidkih Kristallov*, Nauka, Moskva (1982).

32. V. A. Belyakov and S. V. Semenov, *Progr. of* 24^{th} *Int. Liquid Crystal Conf.*, Mainz, p. 92, PIII-148 (2012).

33. V. A. Belyakov and S. V. Semenov, Zh. Eksp. Teor. Fiz. **136**, 797 (2009) [JETP **109**, 687 (2009)].

34. V. A. Belyakov, in *New Developments in Liquid Crystals and Applications*, ed. by P. K. Choundry, Nova Publ., New York (2013), ch. 7, p. 199.